Segmental dynamics of polyurea: Effect of stoichiometry

D. Fragiadakis [a], R. Gamache [b], R.B. Bogoslovov [a], C.M. Roland [a,*]

[a] Naval Research Laboratory, Code 6120, Washington DC 20375-5342, United States
[b] Naval Surface Warfare Center, Research and Technology Dept., Indian Head, MD 20640-5035, United States

ABSTRACT

We study the effect of variations in the soft/hard segment ratio, achieved through stoichiometry changes, in elastomeric polyurea. These variations have a marked effect on the mechanical properties; however, the materials exhibit very similar glass transitions and local segmental relaxation dynamics. The latter differ only at elevated pressure, an increase in hard segment content associated with greater sensitivity to pressure and volume changes. In this respect the polyurea mimics the behavior found recently for an elastomer reinforced with hard filler particles. The resistance to ballistic penetration of the polyurea was unaffected by the stoichiometry variations, consistent with the idea that the impact performance of elastomers is governed by the segmental dynamics rather than properties measured in conventional mechanical tests.

Published by Elsevier Ltd.

1. Introduction

Polyurea is an attractive material for coating applications: it forms *in situ* by the rapid reaction of isocyanates with polyamines, and its mechanical properties can be controlled over a broad range by varying the chemical structure and molecular weight of the components and the relative amounts of isocyanate and amine (i.e., the stoichiometry). Polyureas exhibit a phase separated structure similar to that of segmented polyurethanes, with rigid isocyanate domains (hard phase) embedded within a matrix of flexible chains (soft phase) [1]. Extensive intermolecular hydrogen bonding of polyurea typically leads to high mechanical toughness.

A recent application of elastomeric coatings is to improve the resistance of hard substrates to fragmentation [2] and ballistic penetration [3]. The mechanism of impact mitigation from elastomer coatings is incompletely understood, but an important contribution to the coatings' effectiveness is their ability to transition to the glassy state during the deformation [4]. This means the segmental relaxation times of the coating are on the order of the inverse of the strain rate during impact; this strain rate (estimated as the ratio of the ballistic velocity to polymer thickness) can be as high as 10^5 s^{-1} or more. The viscoelastic rubber-to-glass transition is accompanied by large energy absorption, which thus "toughens" the coating.

Elastomeric polyurea has been successfully employed as an impact coating and in order to understand and optimize

performance, a number of studies have been carried out to characterize its viscoelastic behavior [5–9], as well as efforts to quantify and model the behavior of the coatings [4,10–12]. However, modeling is challenging: on impact, the elastomeric coating is subjected to large strains in combination with large strain rates, and also experiences locally elevated hydrostatic pressure that changes the viscoelastic response.

If an impact-induced glass transition plays a major role in the performance of polyurea coatings, it is important to characterize the segmental dynamics of the soft phase, which controls this transition, as a function of both temperature and pressure. Dielectric spectroscopy is an effective alternative to mechanical measurements of the segmental dynamics, since the former can provide characterization over an extremely wide frequency range and also at elevated pressure. A wide frequency range is especially important for polyureas since they exhibit an extremely broad segmental relaxation, and time–temperature superposition does not apply in the relevant viscoelastic regime [1]. The segmental relaxation times measured using dielectric spectroscopy are expected to be proportional to those derived from dynamic mechanical measurements, although dielectric τ are known to be slightly longer than relaxation times measured mechanically [13].

We recently characterized the viscoelastic properties of a polyurea as a function of temperature and pressure using dielectric spectroscopy [7]. The segmental dynamics was found to conform to a scaling law

$$\tau = f(TV^\gamma) \tag{1}$$

with the material constant $\gamma = 2.35 \pm 0.10$ for polyurea, where V is the specific volume. This scaling allows the prediction for arbitrary

* Corresponding author.
E-mail address: roland@nrl.navy.mil (C.M. Roland).

hydrostatic pressure of the segmental relaxation times, viscosities, and chain relaxation times from ambient pressure data, provided the equation of state is available to interconvert $\tau(T,P)$ and $\tau(T,V)$.

The mechanical properties important for conventional applications are very sensitive to stoichiometry: a 20% change in stoichiometry (corresponding to less than 3% difference in the weight fraction of isocyanate) results in significant qualitative change in the mechanical behavior [5]. It is therefore of interest to examine the effect of stoichiometry on the segmental relaxation of polyurea and its pressure dependence. In this work we study the segmental dynamics of a series of polyureas with different stoichiometries, over a wide range of temperatures (213–353 K) and pressures (0.1 MPa–1 GPa), and assess their conformance to general behaviors known for glass-forming liquids and polymers. Ballistic tests were also carried out for two of the polyureas.

2. Experimental

2.1. Materials

The polyureas were formed by reaction of a polycarbodiimide-modified diphenylmethane diisocyanate (Isonate 143L, Dow Chemical) and poly(tetramethylene oxide-di-p.aminobenzoate) (Versalink P1000, Air Products). The molecular weight given by the manufacturer for the PTMO-amine component is $M = 1238 \pm 72$ g/mol. The components were degassed under vacuum, mixed at room temperature, and molded between Teflon sheets. Curing was carried out at room temperature for 8 h, followed by an additional 12 h at 353 K.

The chemical structures of the diamine and isocyanate and of the resulting polyurea are shown in Fig. 1. The stoichiometry specified by the manufacturer, 96% (diamine/isocyanate by mole), corresponds to a 4:1 ratio of diamine to isocyanate by weight. Three samples with 86, 96 and 106% stoichiometry were prepared, and referred to in the following as PU86, PU96 and PU106. Considering the urea linkage and the phenyl ring of the diamine end group as part of the hard segment, the three polyureas have a hard segment content of 35.4, 33.9 and 32.7% by weight, respectively. Unless otherwise noted, the samples were dried prior to measurement under vacuum for more than 48 h. We refer to such samples are "dry", although trace amounts of residual water may still be present.

Small-angle X-ray scattering profiles of a polyurea with the same composition as PU96 showed peaks at wavenumbers = ~ 0.1 and 0.7 nm^{-1} [1]. These indicate a phase separated morphology of rigid, semi-crystalline isocyanate domains in a polyether matrix, with an average interdomain spacing of 70–80 nm. The shape of the scattering curves is independent of temperature up to 360 K,
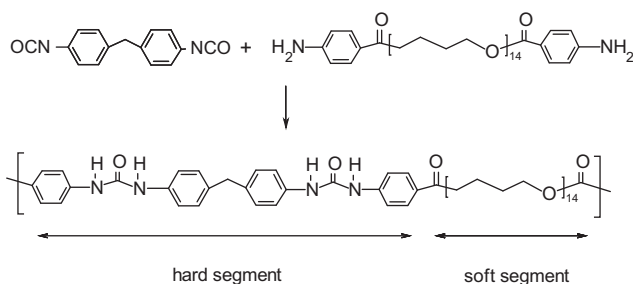
with phase separation, crystal growth, and some ordering of the domains transpiring at higher temperatures. In this study we restrict our measurements to below 354 K and assume, in accord with the reproducibility of dielectric measurements, that the microphase structure remains unchanged within the temperature and pressure range of our experiments.

2.2. Experimental techniques

Dielectric spectroscopy measurements were carried out using parallel plate geometry with the sample in the form of a disk (15–20 mm diameter, 0.2–0.3 mm thick). Spectra were obtained as a function of T and P using a Novocontrol Alpha analyzer (10^{-2}– $\sim 10^{6}$ Hz). For ambient pressure measurements the temperature was controlled using a Delta Design model 9023 oven. For elevated pressure the sample capacitor assembly was contained in a Manganin cell (Harwood Engineering) with pressure applied using a hydraulic pump (Enerpac) in combination with a pressure intensifier (Harwood engineering). Pressures were measured with a Sensotec tensometric transducer (150 kPa resolution). The sample assembly was contained in a Tenney Jr. temperature chamber with control to within ± 0.1 K at the sample.

Differential scanning calorimetry (DSC) measurements were carried out using a TA Instruments Q100 with liquid nitrogen cooling. Samples were equilibrated at 353 K for 15 min, then cooled at 10 K/min (or quenched, in the case of the neat diamine) to 123 K. Heat capacity data were collected during subsequent heating at 10 K/min, with glass transition temperatures defined as the midpoint of the heat capacity jump.

For ballistic tests sheets (19 mm thick) of the polyurea were mounted to the front side of steel plates (5 mm thick "high hard steel", Mil-A-46100). The procedure followed Mil-Std-662F, using 0.50 caliber fragment-simulating projectile having a Rockwell C hardness = 300. The projectiles were shot from a rifled Mann barrel, with the velocity varied by changing the amount of gun powder and measured with a chronograph. The ballistic limit (penetration velocity) was calculated as the midpoint of the lowest velocity for which the projectile penetrated the polyurea/steel assembly and the highest velocity for which complete penetration was not achieved.

3. Results and discussion

3.1. Stress–strain response

Fig. 2 shows stress–strain curves for the three polyureas measured at a strain rate of 0.06 s^{-1} [5]. Despite the small change in hard segment content, the three polyureas have dramatically different mechanical properties, from a highly deformable soft rubber to a rigid, brittle material. The failure strain increases significantly with increasing diamine, while the modulus, yield stress, and failure stress all decrease (Table 1). Note that the 20% difference between the lowest and highest stoichiometry corresponds to a difference of less than 3 wt% in hard segment. Considering the effect of the hard segment domains to be only due to strain-amplification [14], the modulus of the PU should be less than a factor of four higher. In fact these materials have a modulus that is about twenty-fold higher than unreacted soft segment polymer, so that the results cannot be interpreted in terms of a simple filler effect. In polyureas, as in polyurethanes, stoichiometry affects the mechanical response through the degree of crosslinking, the degree and geometry of phase separation, and changes in the extent of hydrogen bonding [15,16].
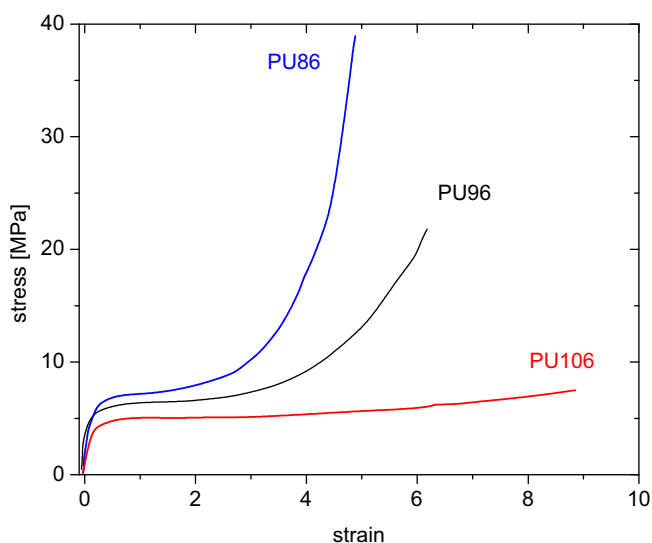

Fig. 1. Structures of the isocyanate, diamine oligomer and the resulting polyurea chain. The isocyanate used also contains a fraction of trifunctional species, not shown here (the average isocyanate functionality is approximately 2.1) resulting in a crosslinked polyurea chain.

Fig. 2. Stress–strain curves for polyureas (from ref. [5]). The extensional strain rate for all tests was 0.06 s^{-1}.
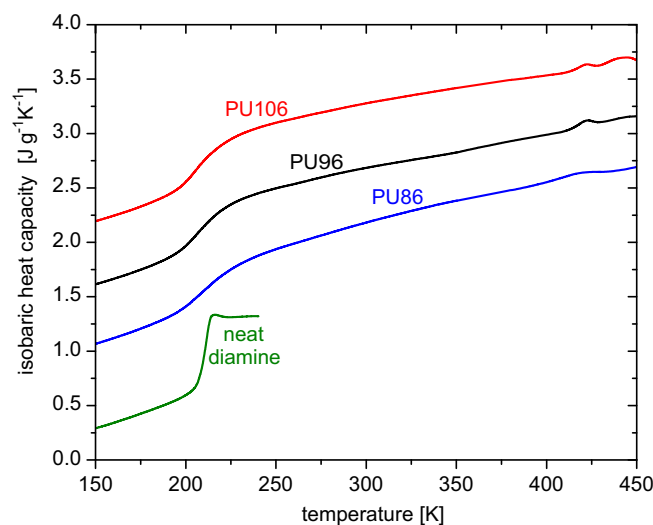

Fig. 3. Heat capacity of polyureas and neat PTMO diamine, measured during heating at 10 K/min following cooling at 10 K/min for polyureas and following quenching for the diamine. The glass transition of the soft segment is seen around 210 K and that order–disorder transition around 423 K. The ordinate values have been shifted for clarity.

3.2. Calorimetric glass transition

Despite the significant differences in mechanical behavior, the calorimetric glass transition of the soft phase, shown in Fig. 3, is very similar for the three polyureas. The glass transition temperatures differ by only 1–2 K and are close to that of the unreacted diamine, indicating a high degree of phase separation. The heat capacity increment at T_g increases slightly with increasing soft segment content (Table 2). The glass transition in the polyureas is extremely broad, with a $\Delta T = T_{end} - T_{onset}$ of *ca.* 30–35 K for all three compositions, compared to 4 K for the diamine. This indicates that the dynamics of the soft phase is extremely heterogeneous.

Two factors contribute to this heterogeneity. The first is compositional, due to the presence of isocyanate segments within the soft phase. Their concentration should be especially significant near the phase boundaries, leading to a diffuse interface. The second is slowing down of the segmental dynamics of PTMO chains in proximity to rigid isocyanate domains, due either to anchoring of the chains or to a physical effect. This physical effect refers to the fact that the dynamics near T_g are cooperative, having a length scale of a few nm. This is a significant fraction of the spacing between the isocyanate domains; consequently, some fraction of the soft phase will be slowed, contributing to more heterogeneous dynamics and a broader glass transition.

At higher temperatures ($\sim$423 K) there is a weak endothermic peak associated with dissolution of the domains [1]. This order–disorder transition, and by inference the stability of the phase morphology, appear to be unaffected by the changes in stoichiometry.

3.3. Dielectric relaxation

Fig. 4 shows representative dielectric loss spectra for dry PU96 at ambient pressure. At low temperatures, there is a single

relaxation (α-process), extremely broad on the low-frequency side. With increasing temperature a second loss maximum (α'-process) is resolved at lower frequencies. At the lowest frequencies a pronounced increase of ε'' is observed; this is due to dc conductivity and interfacial polarization at the boundaries between soft and hard domains, which have different dielectric constants and conductivities.

Spectra for dry PU86 and PU106, shown in Fig. 5 for ambient pressure, are qualitatively similar to PU96. However the α'-process is suppressed in PU86 and much more pronounced in PU106, compared to PU96. The change in relaxation strength of the α'-process is obviously much larger than the 1–2 wt% change in soft segment content between samples.

The dielectric loss spectra were fit with the sum of a power law (to describe the low-frequency conductivity) and a Havriliak–Negami [17] term for each relaxation. The obtained relaxation times τ_α and $\tau_{\alpha'}$, are plotted against inverse temperature in Fig. 6. Also included in the plot are dielectric τ_α from ref. [4] for a polyurea of the same composition containing 0.8 wt% water, and mechanical τ_α from ref. [1]. The glass transition temperature measured using DSC is indicated in the figure. The α-process shows the non-Arrhenius temperature dependence expected for segmental relaxation. The α'-process, observed as a separate peak only in dry samples, is 3 orders of magnitude slower with essentially the same temperature dependence. At ambient pressure the relaxation times for both processes are equal to within experimental error, for all three polyureas.

The temperature dependence of τ for both relaxations can be described using the Vogel–Fulcher equation [18]

$$\tau = \tau_0 \exp\left(\frac{B}{T - T_0}\right) \tag{2}$$

Table 1
Mechanical properties and ballistic penetration results.

	PU86	PU96	PU106
Secant modulus ($\varepsilon = 0.3$) [MPa]	21.9	17.8	15.5
Tensile strength [MPa]	39.0	22.7	7.5
Failure strain (%)	490	625	890
Ballistic limit[a] [m/s]	893 ± 6	900 ± 2	–

[a] Mil-Std-662F.

Table 2
Calorimetric glass transition temperature, width of the glass transition and heat capacity increment for the three polyureas and the neat diamine.

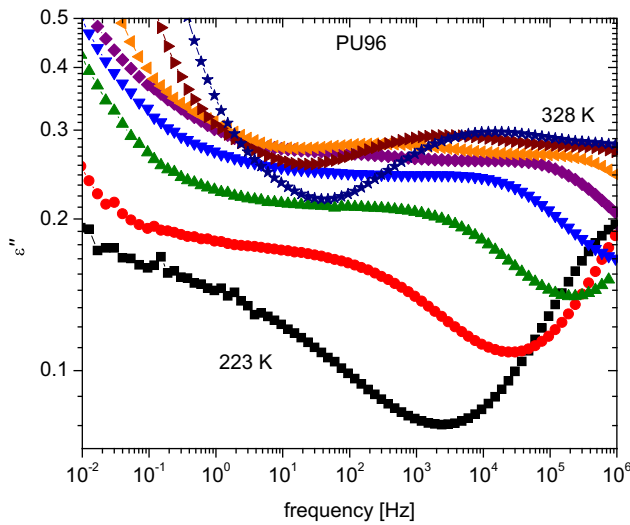|	PU86	PU96	PU106	Neat diamine
T_g(DSC) [K]	209.8 ± 2.0	208.3 ± 2.0	207.6 ± 2.0	210.2 ± 1.0
ΔT(DSC) [K]	34 ± 5	29 ± 3	27 ± 3	4 ± 1
Δc_p(DSC) [Jg^{-1}K^{-1}]	0.42 ± 0.02	0.46 ± 0.02	0.49 ± 0.02	0.67 ± 0.02

Fig. 4. Representative dielectric loss spectra for dry PU96 at $P = 0.1$ MPa, for temperatures from $T = 223$ to 328 K in steps of 15 K.

with the fit parameters τ_0, B, and T_0 (from a simultaneous description of $\tau(T)$ for all three polyureas) given in Table 3. The extrapolated temperature for which $\tau_\alpha = 100$ s ($T = 207$ K) is in good agreement with the calorimetric glass transition temperature, and the α-relaxation times are close to, but somewhat longer than, those previously determined from dynamic mechanical measurements [1]. For the α'-process, on the other hand, the extrapolated T for which $\tau_{\alpha'} = 100$ s is 227 K, at which temperature the calorimetric glass transition is already complete (for all three polyureas the end temperature of the DSC glass transition is 224 ± 3 K). Mechanical spectra show no relaxation component with a relaxation time corresponding to τ_α. The origin of this α'-process will be discussed below.

3.4. Effect of water content on dielectric relaxation

Polyurea is hygroscopic, having a water content that depends on the ambient humidity. For reference, all three polyureas were
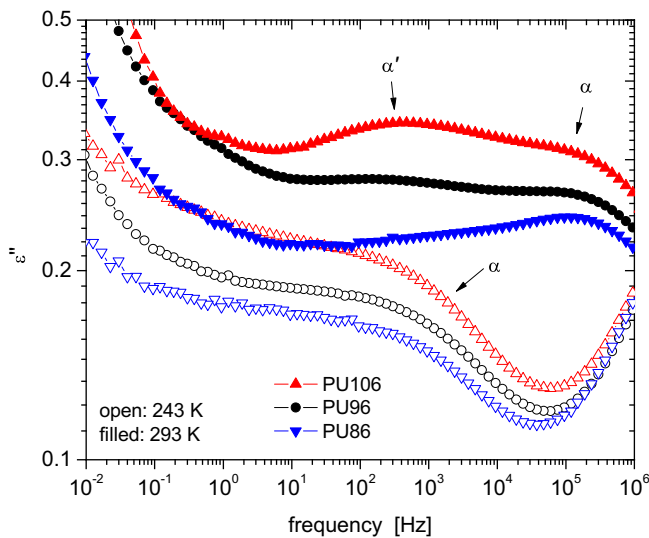

Fig. 5. Effect of stoichiometry on dielectric relaxation: dielectric loss spectra for dry PU86, PU96 and PU106 at $P = 0.1$ MPa and $T = 243–293$ K.
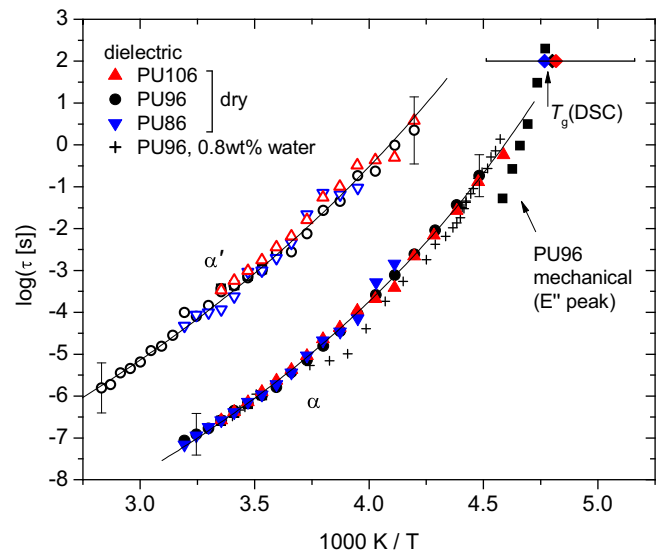

Fig. 6. Temperature dependence of the relaxation times for the α- (segmental) and α'-processes of the polyureas measured at ambient pressure. Also shown are the calorimetric T_g (assuming an enthalpy relaxation time of 100 s, the horizontal bar indicates the approximate onset and end of the transition); dielectric τ_α data from ref. [4] for PU96 containing 0.8 wt% water; and segmental relaxation times for PU96 from ref. [1], determined as the inverse of the frequency of the peak in the mechanical loss modulus. The lines are fits of Eq. (1).

determined to have *ca.* 0.8 wt% water at 50% relative humidity and 2.4 wt% at 100% relative humidity. The dielectric response is very sensitive to water content, as shown in Fig. 7 for PU96. For the dry polyurea, the α'-process is clearly resolved as a loss maximum around 3 decades slower than the α-process. With increasing water content, the relaxation time of the α-process remains constant, but the α'-process becomes progressively faster, ultimately merging with the α-process into a single loss peak. At least up to 0.8 wt% water, the α-relaxation time is independent of water content to within experimental error over the entire frequency range (Fig. 6).

3.5. Origin of the α'-process

A comparison of relaxation times for PU96 obtained using different techniques (Fig. 6) suggests that both the mechanical and calorimetric glass transitions correspond to the α-process, while the α' peak has no calorimetric or mechanical signature. The relaxation strength of the α'-process is quite sensitive to stoichiometry and its relaxation time increases with water content.

What, then, is the origin of the α'-process? One possibility would be interfacial polarization; i.e., accumulation of mobile ions at the interfaces between the more conductive soft phase and the less conductive hard phase. However, the relatively low relaxation strength, a sensitivity to small changes in the stoichiometry, and its merging with the α-process at higher water content make this interpretation of the α'-process unlikely. Such interfacial polarization was indeed observed at lower frequencies, in the region of the spectrum dominated by conductivity.

Table 3
α and α' relaxation parameters for the polyureas[a] at $P = 0.1$ MPa.

	$\log(\tau_0 \, [s])$	B [K]	T_0 [K]	T [K] at $\tau = 100$ s
α-Process	12.9 ± 0.8	2680 ± 470	133 ± 10	206.7 ± 2.0
α'-Process	11.5 ± 0.7	3497 ± 500	120 ± 10	227.0 ± 3.0

[a] Simultaneous fit to relaxation times of all three polyureas.

The sensitivity of the relaxation strength to stoichiometry suggests that the α'-process is related to unreacted ends of the diamine component. The chain ends of the diamine, containing a primary amine and carbonyl group, are extremely polar. This is evidenced by the fact that the static dielectric constant at 293 K of the neat diamine is 11, compared to $\varepsilon' = 5$ for a PTMO of equal molecular weight. When the diamine is incorporated into the polyurea, most of the chain ends react with isocyanate to form urea linkages. This attachment to the rigid isocyanate domains largely immobilizes these chain ends, so they effectively become part of the hard domain. Any unreacted diamine moieties remain dissolved in the soft phase and due to their polar nature act as a dielectric probe [19], accentuating in the spectrum the response of their surroundings in the highly heterogeneous microstructure. It is reasonable to assume that in the dry polyurea, the chain ends migrate toward the interface between the soft and hard phases, where the chemically similar reacted chain ends are located. Close to the interface we expect the dynamics to be slowed due to anchoring on the hard domains and/or partial mixing, thus giving rise to the slower α' peak. With the addition of water, the increasing polarity of the PTMO region likely drives the chain ends away from the interface, leading to a more homogeneous distribution in the PTMO phase.

An alternative explanation is that the water molecules screen the relatively weak hydrogen bonds between the isocyanate and PTMO phase (though they cannot break the much stronger bonds between isocyanate segments), leading to more homogeneous dynamics in the latter. However, more homogeneous dynamics would also lead to a narrower calorimetric glass transition. This is not observed; the width of the calorimetric T_g was almost unchanged up to water contents of 0.8 wt%. This supports our interpretation of the α' peak as reflecting unreacted diamine.

3.6. Effect of pressure on τ_α

Although the segmental dynamics are independent of stoichiometry at $P = 0.1$ MPa, this is not the case at elevated pressure. Fig. 8 shows the pressure dependence of the segmental relaxation times for four measurement temperatures from 297 to 350 K. The variation of $\log\tau_\alpha$ with pressure is roughly linear. At low pressures the

relaxation times of the three polyureas are essentially equivalent, in agreement with the ambient pressure data of Fig. 6. However, with increasing pressure the τ_α diverge by more than an order of magnitude.

A linear dependence of $\log\tau_\alpha$ on P can be quantified using the activation volume [20]

$$\Delta V^{\#} = \frac{RT}{\log e} \frac{\partial \log\tau_\alpha}{\partial P}\bigg|_T \tag{3}$$

Here R is the gas constant and e the base of the natural logarithm. The values of $\Delta V^{\#}$ determined from the slopes of linear fits to $\log \tau(P)$ are shown in Fig. 9. $\Delta V^{\#}$ decreases systematically with increasing temperature, as found previously for PU96; this is the general behavior of liquids and polymers [20]. In addition, with increasing hard segment content the activation volume increases significantly (more than 40% for a change of less than 3 wt% hard segment content); that is, the dynamics becomes more pressure-sensitive.

3.7. Thermodynamic scaling

The activation volumes describe the effect of pressure on the dynamics; a more complete description takes into account the effects of both volume and of temperature on τ_α. It has been shown that the relaxation time for many non-associated liquids and polymers obeys the scaling law (Eq. (1)) [21–23], where the material-specific constant γ, related to the steepness of the inter-molecular repulsive potential [24,25], assumes values between 2 and 8 [20]. Larger γ reflects a greater contribution of volume, relative to that of temperature, to the dynamics. This scaling relation also holds over limited ranges of T and P for some hydrogen-bonded and ionic liquids, but fails for strongly hydrogen-bonded systems due to the nontrivial change of chemical structure with thermodynamic conditions [26, 27]. For polyurea, with a complex heterogeneous morphology and extensive hydrogen bonding, it is not obvious that the scaling property should hold. However, τ_α for PU96 (with a water content of 3.5%) was recently found to obey Eq. (1) with value of $\gamma = 2.35 \pm 0.1$, which is low, characteristic of associating systems [7]. In Fig. 10 we plot the relaxation times
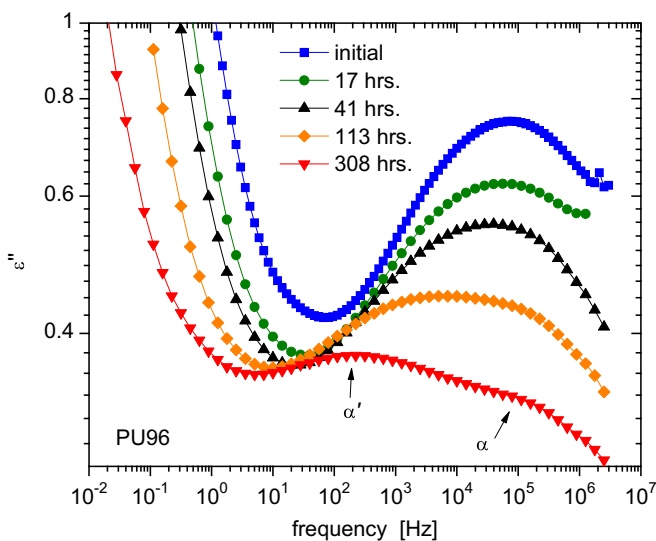

Fig. 7. Effect of water content on dielectric relaxation: dielectric loss spectra at 298 K for PU96 containing 0.8 wt% water, and of the same sample after exposure to dry nitrogen for 17, 42, 113 and 308 h.
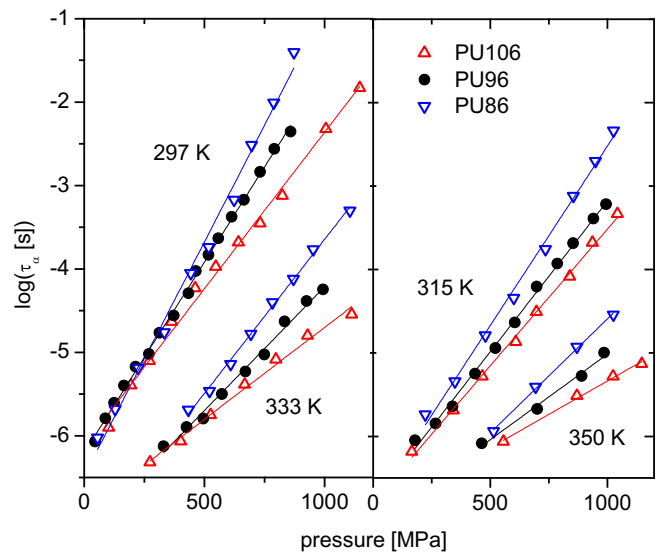

Fig. 8. Pressure dependence of the segmental relaxation times of PU86, PU96, and PU106 at the indicated temperatures. The slopes of the fitted lines yield the activation volumes displayed in Fig. 9.

versus the scaling variable TV^γ for the three polyureas. We obtain good superpositioning, with an exponent γ that increases from 2.08 ± 0.15 to 2.45 ± 0.15 with increasing amount of hard segment. The value for dry PU96 is 2.24 ± 0.15, equal within experimental error to that reported in ref. [7] for PU96, containing 3.5 wt% water. This suggests that in the entire range from dry to saturated polyurea, water content affects the pressure sensitivity of the segmental dynamics only weakly, if at all.

It is not clear why the pressure/volume sensitivity of the segmental relaxation should increase with the relative amount of isocyanate. One possibility is a decrease of the hydrogen bonding within the soft phase. In polyglycols this has been shown to increase the volume sensitivity of the dynamics [27]. With higher hard segment content there are fewer unreacted PTMO-amine chain ends, and thus fewer of the amine and carbonyl groups that H-bond within the soft phase.

An interesting parallel can be drawn to a recent study of poly(vinyl acetate) (PVAc) containing 100 nm silica particles [28]. The glass transition temperature and segmental relaxation times at ambient pressure of the PVAc were unchanged up through silica volume concentrations of 28% by weight. However, the volume sensitivity of the segmental dynamics, as reflected in the parameter γ, became stronger with increasing silica content, especially in the vicinity of the percolation threshold. This suggests that a general characteristic of polymer segmental dynamics is an increasing volume sensitivity in the presence of small particle fillers (or hard segments).

3.8. Isochronal superpositioning

Although the shape of the α-relaxation function (reflecting the distribution of segmental relaxation times) typically changes with temperature and pressure, it has been shown for a variety of systems that the peak shape is invariant for different combinations of temperature and pressure that correspond to the same relaxation time [29,30]. Fig. 11 shows three sets of dielectric spectra, each set associated with a particular fixed value of the segmental relaxation times of PU96 (very similar behavior is observed for PU106 and PU86). Curves corresponding to the same τ_α superimpose well in the frequency region of the segmental process, even

Fig. 10. Segmental (α) relaxation times plotted against TV^γ, for the values of the exponent γ indicated. γ increases with increasing hard segment content.

though the shapes of the curves for different τ_α are very different. At lower frequencies the superposition breaks down as conductivity and interfacial polarization dominate the spectra.

3.9. Impact resistance

Table 1 compares the ballistic limit of steel plates with PU86 and PU96 coatings on the front (impact) side. Despite their very significant difference in mechanical behavior, particularly failure properties, the resistance to impact penetration of the two materials is equivalent within the experimental error. This result is in accord with previous studies indicating that for high strain rate deformations (ca. $10^4 \, s^{-1}$ and higher), the segmental dynamics govern the response of an elastomer [4,12,31]. The changes in stoichiometry do not effect any substantial change in the intensity of the α-relaxation process, given the small changes (couple
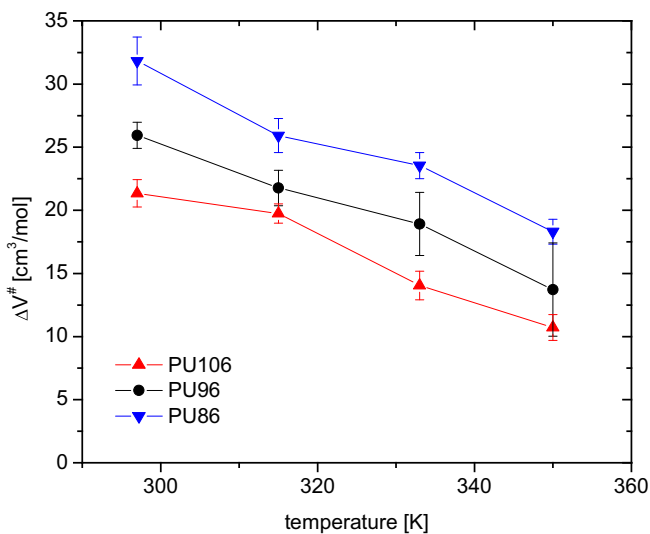

Fig. 9. Activation volumes for the segmental relaxation of PU86, PU96 and PU106 as a function of temperature. The activation volume increases with decreasing temperature and increasing hard segment content.
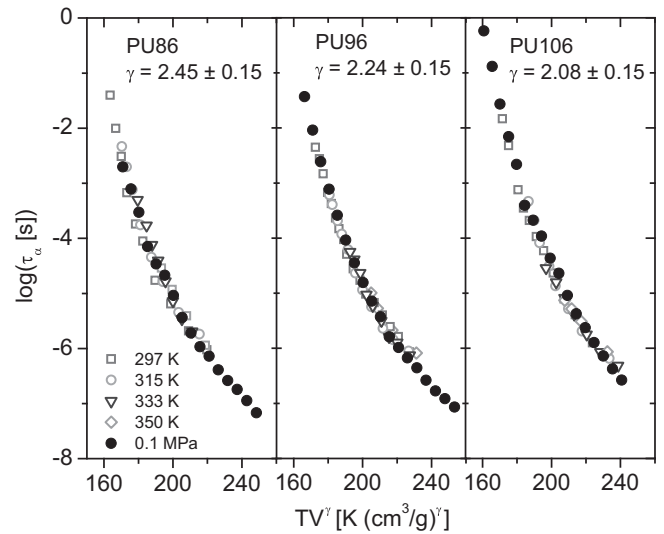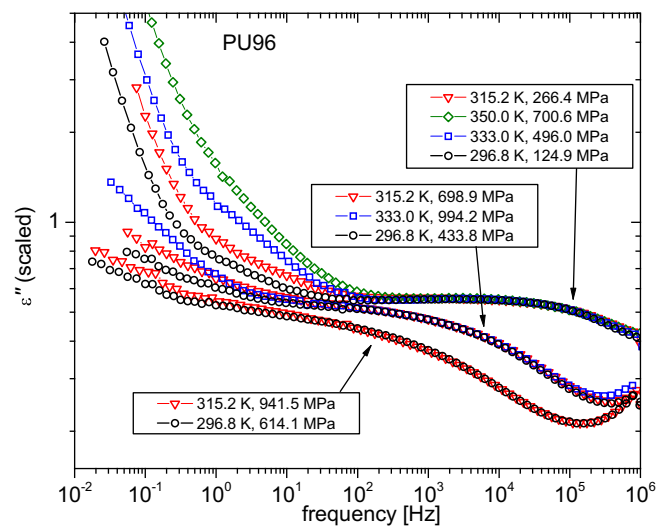

Fig. 11. Dielectric loss spectra for PU96, for which the segmental relaxation time is equal to a common value respectively of 7.8×10^{-5} s, 1.6×10^{-5} and 1.3×10^{-6} (from left to right). The spectra were shifted along the vertical axis, and slightly along the horizontal axis, to superimpose the peaks. The superposition breaks down in the low-frequency region where conductivity and interfacial polarization dominate.

percent) in the quantity of the soft segment phase. Thus, the energy dissipation in the two coatings is similar. There are modest changes in the time scale of the soft segment dynamics, especially at high-pressure (the impact loading likely raises the local hydrostatic pressure, but the magnitude of this effect is unknown). However, since the glass transition of the polyurea is very broad, any difference in τ_α between the PU86 and PU96 do not prevent the impact frequency from falling within the dispersion of the α-relaxation process for either material.

4. Summary

The soft segment segmental relaxation times were measured as a function of temperature and pressure for a series of polyureas with varying stoichiometry. The variations in the polyurea chemistry engendered large differences in mechanical properties. However, the segmental relaxation times and calorimetric T_g at ambient pressure were unaffected by stoichiometry. Surprisingly, the pressure sensitivity of the segmental relaxation time did increase significantly with increasing hard segment content, potentially affecting the performance of polyurea coatings in impact applications associated with localized pressure elevation. The polyureas conform to the general behaviors found to apply to simpler polymers and glass-forming liquids: invariance of the distribution of relaxation times at fixed τ_α, and the scaling of the relaxation times; i.e., their superposition when plotted as a function of TV^γ with γ a material constant. The exponent γ increases with increasing hard segment content indicating increased volume sensitivity of the dynamics. Using this scaling property the segmental relaxation times and related properties can be predicted from knowledge of the exponent γ and the properties at ambient pressure. The variation in soft segment content with changes in stoichiometry is small (few percent) and thus the ballistic impact response, which is governed by the local segmental dynamics, is equivalent for the polyureas. This emphasizes the irrelevance of conventional (slow rate) mechanical properties for elastomers used in applications such as ballistic protection. With regard to polyurea herein, better performance requires more substantial changes in the structure and morphology than can be achieved by stoichiometry variations.

Acknowledgments

References

[1] Pathak JA, Twigg JN, Nugent KE, Ho DL, Lin EK, Mott PH, et al. Macromolecules 2008;41(20):7543–8.
[2] Davidson JS, Fisher JW, Hammons MI, Porter JR, Dinan RJ. Journal of Structural Engineering 2005;131(8):1194–205.
[3] Tekalur SA, Shukla A, Shivakumar K. Composite Structures 2008;84(3):271–81.
[4] Bogoslovov RB, Roland CM, Gamache RM. Applied Physics Letters 2007;90(22):3.
[5] Roland CM, Twigg JN, Vu Y, Mott PH. Polymer 2007;48(2):574–8.
[6] Yi J, Boyce MC, Lee GF, Balizer E. Polymer 2006;47(1):319–29.
[7] Roland CM, Casalini R. Polymer 2007;48(19):5747–52.
[8] Jiao T, Clifton RJ, Grunschel SE. High strain rate response of an elastomer. In: Furnish MD, Elert M, Russell TP, White CT, editors. Conference of the American physical society topical group on shock compression of condensed matter, vol. 845. Baltimore, MD: Amer Inst Physics; 2005. p. 809–12.
[9] Shim J, Mohr D. International Journal of Impact Engineering 2009;36(9): 1116–27.
[10] Amirkhizi AV, Isaacs J, McGee J, Nemat-Nasser S. Philosophical Magazine 2006;86(36):5847–66.
[11] Li CY, Lua J. Materials Letters 2009;63(11):877–80.
[12] Roland CM, Fragiadakis D, Gamache RM. Composite Structures, in press, doi: 10.1016/j.compstruct.2009.09.057.
[13] McCrum NG, Read BE, Williams G. In: Dover, editor. Anelastic and dielectric effects in polymeric solids. New York: Dover Publications; 1991.
[14] Guth E. Journal of Applied Physics 1945;16(1):20–5.
[15] Stanford JL, Still RH, Wilkinson AN. Polymer 1995;36(18):3555–64.
[16] Martin DJ, Meijs GF, Renwick GM, McCarthy SJ, Gunatillake PA. Journal of Applied Polymer Science 1996;62(9):1377–86.
[17] Havriliak S, Negami S. Journal of Polymer Science Part C-Polymer Symposium 1966;(14PC)::99.
[18] Kremer F, Schönhals A. Broadband dielectric spectroscopy. Berlin; New York: Springer; 2003.
[19] Wubbenhorst M, van den Berg O, Picken SJ, Jager WF. Journal of Non-Crystalline Solids 2005;351(33–36):2694–702.
[20] Roland CM, Hensel-Bielowka S, Paluch M, Casalini R. Reports on Progress in Physics 2005;68(6):1405–78.
[21] Casalini R, Roland CM. Physical Review E 2004;69(6):3.
[22] Alba-Simionesco C, Cailliaux A, Alegria A, Tarjus G. Europhysics Letters 2004;68(1):58–64.
[23] Dreyfus C, Le Grand A, Gapinski J, Steffen W, Patkowski A. European Physical Journal B 2004;42(3):309–19.
[24] Roland CM, Feldman JL, Casalini R. Journal of Non-Crystalline Solids 2006;352:4895–9.
[25] Coslovich D, Roland CM. Journal of Physical Chemistry B 2008;112(5): 1329–32.
[26] Roland CM, Bair S, Casalini R. Journal of Chemical Physics 2006;125(12):8.
[27] Roland CM, Casalini R, Bergman R, Mattsson J. Physical Review B 2008;77(1):4.
[28] Bogoslovov RB, Roland CM, Ellis AR, Randall AM, Robertson CG. Macromolecules 2008;41(4):1289–96.
[29] Roland CM, Casalini R, Paluch M. Chemical Physics Letters 2003; 367(3–4):259–64.
[30] Ngai KL, Casalini R, Capaccioli S, Paluch M, Roland CM. Journal of Physical Chemistry B 2005;109(37):17356–60.
[31] Roland CM. Rubber Chemistry and Technology 2006;79(3):429–59.